Volume 19
Number 10
October 1980

Inorganic Chemistry

© Copyright 1980 by the American Chemical Society

Contribution from the Department of Chemistry, University of Oklahoma, Norman, Oklahoma 73019,
and the Chemistry Department, Babes-Bolyai University, R3400 Cluj-Napoca, Romania

Oxy and Thio Phosphorus Acid Derivatives of Tin. 4. Diorganotin(IV) Bis(dithiophosphate) Esters

J. L. LEFFERTS, K. C. MOLLOY, J. J. ZUCKERMAN,* I. HAIDUC,* M. CURTUI, C. GUTA, and D. RUSE

Received December 26, 1979

Eleven dimethyl- and diphenyltin bis(dithiophosphate) esters, $R_2Sn[S_2P(OR')_2]_2$, where R = CH_3 and R′ = CH_3, C_2H_5, *n*-C_3H_7, and *i*-C_3H_7 and where R = C_6H_5 and R′ = CH_3, C_2H_5, *n*-C_3H_7, *i*-C_3H_7, *n*-C_4H_9, *i*-C_4H_9, and C_6H_5, are synthesized in high yield by the reaction of the diorganotin dichlorides with the ammonium, sodium, or potassium salts of the dithiophosphoric acid ester or by the condensation of the diorganotin(IV) oxide with the *O,O′*-diorganodithiophosphoric acid in benzene to release water which is distilled azeotropically to drive the reaction forward. The products are colorless, crystalline solids or oils, soluble in organic solvents. Infrared band assignments can be made in the case of the ν(CO) (1150–1145 cm^{-1}), ν(POR) (1025–985 cm^{-1}), and $\nu(PS_2)$ (660–610 cm^{-1}) modes, but the $\nu_{sym}(PS_2)$ absorptions obscure the important ν(SnC) modes. NMR $|^2J(^{119}Sn-C-^1H)|$ coupling constants of 79–80 Hz for the methyltin derivatives are consistent with six-coordinated diorganotin species in solution, and mass spectral data are consistent with monomers. Tin-119m Mössbauer isomer shift (IS) values (1.35–1.47 mm s^{-1}), ρ [ratio of quadrupole splitting (QS) to IS] (2.18–2.65), and QS values (3.12–3.67 mm s^{-1}) specify diorganotin(IV) complexes in a six-coordinated, trans-octahedral geometry. Available C–Sn–C angle data for the ethyl (135°) and isopropyl (180°) ester derivatives allow the correlation with QS to be calibrated, and this relationship is used to predict the angles in the other diphenyltin systems studied. The ethyl and *n*-propyl ester derivatives behave roughly equivalently in a variable-temperature Mössbauer study, where the slope of the temperature dependence of the log of the resonance area is consistent with a structure consisting of noninteracting, monomeric molecules, and the two ester analogues are predicted to be approximately isostructural with a C–Sn–C angle of 135°. The isopropyl ester derivative is by contrast tightly packed into a strongly bound lattice in which short sulfur–sulfur atom contacts play an important role, and this is reflected in a much diminished slope.

In other portions of this series of papers we have described the synthesis of the triorganotin(IV) dithiophosphate esters[1] and the X-ray crystal structures of (*O,O′*-diethyl dithiophosphato)triphenyltin(IV), $(C_6H_5)_3SnS_2P(OC_2H_5)_2$, a rare monodentate dithiophosphate derivative,[2] bis(*O,O′*-diphenyl dithiophosphato)tin(II), $Sn[S_2P(OC_6H_5)_2]_2$, a bicyclic dimer held together in part by η^6-C_6H_5 to tin(II) lone-pair interactions,[3] and bis(*O,O′*-diisopropyl dithiophosphato)diphenyltin(IV), $(C_6H_5)_2Sn[S_2P(OC_3H_7\text{-}i)_2]_2$, a trans-octahedral monomer tightly packed into a "virtual polymer" lattice.[4] One goal of these studies is to incorporate into the same molecule biocidal organotin moieties[5,6] with organophosphorus ligands which also show powerful biological activity. The resulting dual-acting compounds could potentially exhibit a still stronger and more lasting effect and circumvent problems of the development of tolerance to each molecular part. In this paper we extend the series to report the synthesis of several diorganotin(IV) bis(dithiophosphate) esters.

Table I. Diorganotin(IV) Bis(dithiophosphate) Esters

R	R′	prepn	yield, %	mp, °C	%P calcd	%P found
CH_3	CH_3	1, 2	50, 68	82	13.40	12.80
CH_3	C_2H_5	1, 2	80, 71	32–33	11.90	11.10
CH_3	*n*-C_3H_7	1, 2	82, 60	oil	10.80	9.80
CH_3	*i*-C_3H_7	1, 2	65, 40	32–3	10.80	9.60
C_6H_5	CH_3	1	62	118	10.55	10.50
C_6H_5	C_2H_5	1	82	53	9.63	8.95
C_6H_5	*n*-C_3H_7	1	70	41	8.86	8.47[a]
C_6H_5	*i*-C_3H_7	1	88	108	8.86	8.64[b]
C_6H_5	*n*-C_4H_9	1	33	ca. 29	8.22	7.46
C_6H_5	*i*-C_4H_9	3	66	82.5–83.5	*c*	
C_6H_5	C_6H_5	3	70	145.5–146.5	*d*	

[a] Anal. Calcd: S, 18.3 Found: S, 18.0. [b] Anal. Calcd: S, 18.3. Found: S, 18.0. [c] Anal. Calcd: C, 44.50; H, 6.15. Found: C, 44.74; H, 6.33. [d] Anal. Calcd: C, 51.75; H, 3.63. Found: C, 51.52; H, 3.49.

Experimental Section

Organotin starting materials were of commercial grade and were used without further purification. The dithiophosphoric acids and their sodium, potassium, and ammonium salts were prepared by literature methods described in part 1 of this series.[1] Carbon and hydrogen analyses were performed by Galbraith Laboratories, Inc., Knoxville, Tenn.

Infrared spectra were recorded on a Beckman 4250 spectrometer as Nujol mulls on KBr plates and polyethylene film. Mass spectra were recorded on a Hewlett-Packard 5985B mass spectrometer. Tin-119m Mössbauer spectra were recorded on a Ranger Engineering

---

*To whom correspondence should be addressed: J.J.Z., University of Oklahoma; I.H., Babes-Bolyai University.

(1) Lefferts, J. L.; Molloy, K. C.; Zuckerman, J. J.; Haiduc, I.; Guta, C.; Ruse, D. *Inorg. Chem.* **1980**, *19*, 1662.
(2) Molloy, K. C.; Hossain, M. B.; van der Helm, D.; Zuckerman, J. J.; *Inorg. Chem.* **1979**, *18*, 3507.
(3) Lefferts, J. L.; Hossain, M. B.; Molloy, K. C.; van der Helm, D.; Zuckerman, J. J. *Angew. Chem., Int. Ed. Engl.* **1980**, *19*, 309.
(4) Molloy, K. C.; Hossain, M. B.; van der Helm, D.; Zuckerman, J. J.; Haiduc, I. *Inorg. Chem.* **1980**, *19*, 2041.
(5) Zuckerman, J. J. *Adv. Chem. Ser.* **1976**, No. 157.
(6) Zuckerman, J. J.; Reisdorf, R. P.; Ellis, H. V., III; Wilkinson, R. R. *ACS Symp. Ser.* **1978**, *No. 82*, 388.

0020-1669/80/1319-2861$01.00/0 © 1980 American Chemical Society

Table II. Tin-119 Mössbauer Data for $R_2Sn[S_2P(OR')_2]_2$ at 77 K

R	R′	IS[a,b]	QS[a,c]	Γ_+[a,c]	Γ_-[a,c]	ρ[d]
C_6H_5	CH_3	1.35	3.34	1.07	1.47	2.47
C_6H_5	C_2H_5	1.41	3.12	1.07	1.20	2.21
C_6H_5	*n*-C_3H_7	1.42	3.22	1.11	1.16	2.27
C_6H_5	*i*-C_3H_7	1.40	3.67	1.14	1.24	2.62
C_6H_5	*i*-C_4H_9	1.43	3.62	1.15	1.28	2.53
C_6H_5	C_6H_5	1.47	3.21	1.40	1.80	2.18
CH_3	CH_3	1.43	3.35	1.09	1.30	2.34
CH_3	C_2H_5	1.44	3.34	1.32	1.62	2.32

[a] In mm s^{-1}. [b] ±0.02 mm s^{-1}. [c] ±0.05 mm s^{-1}. [d] ρ = QS/IS.

constant-acceleration spectrometer equipped with an NaI scintillation counter and using $Ca^{119m}SnO_3$ (New England Nuclear Corp.) as the source and $Ca^{119}SnO_3$ as standard reference material for zero velocity. Velocity calibration was based upon β-tin. Standard, nonlinear, least-squares techniques were used to fit the data to Lorentzian curves. The Ranger Engineering variable-temperature liquid-nitrogen dewar and controller used in these studies is regulated by a variable-bridge, silicon-controlled-rectifier circuit and is accurate to ±1 K. Raman data were taken on a Spex Ramalog 5 laser Raman spectrometer.

The compounds studied are listed with the preparatory method used and their yields, melting points, and microanalytical data in Table I. Tin-119m Mössbauer data are listed in Table II and proton magnetic resonance, infrared, and mass spectrometric data in Tables III–V. Four typical preparations are described in detail below.

Bis(*O,O′*-dimethyl dithiophosphato)diphenyltin(IV), $(C_6H_5)_2Sn[S_2P(OCH_3)_2]_2$. Diphenyltin dichloride (1.72 g, 0.005 mol) in diethyl ether (50 mL) was added to a solution of ammonium dimethyl dithiophosphate (1.75 g, 0.01 mol) in anhydrous ethanol (110 mL), and the mixture was allowed to reflux for ca. 0.5 h. The resulting precipitate was removed by filtration and the filtrate slowly concentrated to give the product as white crystals (1.80 g, 62%), mp 118 °C.

Other similar compounds prepared by this method, with the amounts of reagents and yields, are tabulated in Table VI.

Bis(*O,O′*-dimethyl dithiophosphato)dimethyltin(IV), $(CH_3)_2Sn[S_2P(OCH_3)_2]_2$. Metallic sodium (0.46 g, 0.02 mol) was dissolved in absolute ethanol (50 mL) and the resulting solution treated with dimethyldithiophosphoric acid (3.16 g, 0.02 mol). A solution of dimethyltin dichloride (2.20 g, 0.02 mol) in absolute methanol was added to form a white precipitate of NaCl which was separated by filtration. The filtrate was concentrated to give a white crystalline product (3.15 g, 68%), mp 82 °C.

Other compounds prepared by this method are listed in Table VII.

Bis(*O,O′*-diphenyl dithiophosphato)diphenyltin(IV), $(C_6H_5)_2Sn[S_2P(OC_6H_5)_2]_2$. A suspension of diphenyltin(IV) oxide (2.89 g, 0.01 mol) and diphenyldithiophosphoric acid (5.64 g, 0.02 mol) in benzene (100 mL) was allowed to reflux for ca. 1 h, and the water formed in the reaction was separated azeotropically by a Dean and Stark apparatus. The cooled solution was filtered to remove trace amounts of solid and concentrated to ca. 10 mL. The solid that precipitated was redissolved in hot toluene, crystallized at 0 °C, filtered, and washed with hexane to yield a cream-colored solid. Recrystallization from hexane–toluene (3:1) yielded 5.82 g (70%) of pure product, mp 145.5–146.5 °C.

Bis(*O,O′*-diisobutyl dithiophosphato)diphenyltin(IV), $(C_6H_5)_2Sn[S_2P(O\text{-}i\text{-}C_4H_9)_2]_2$. Diphenyltin(IV) oxide (2.89 g, 0.01 mol) and diisobutyldithiophosphoric acid (4.84 g, 0.02 mol) were refluxed together in benzene (100 mL) for 12 h, as outlined above. Concentration of the resulting solution afforded a colorless oil, which was recrystallized from hexane at −78 °C to give the crude product as a white solid. Subsequent recrystallization from hexane at 0 °C produced 5.02 g (66%) of a pure, white crystalline product, mp 82.5–83 °C.

Results and Discussion

The diorganotin(IV) bis(dithiophosphate) esters can be synthesized in high yield by the action of the ammonium salt

Table III. ^1H NMR Data for $R_2Sn[S_2P(OR')_2]_2$[a,b]

R	R′	chemical shifts (δ) and coupling constants (*J*, Hz)
CH_3	CH_3	3.70, d, 12 H (OCH_3), $|^3J(^{31}\text{P-O-C-}^1\text{H})| = 15.5$; 1.52, s, 6 H (Sn–$CH_3$), $|^2J(^{119,117}\text{Sn-C-}^1\text{H})| = 80.0, 76.0$
CH_3	C_2H_5	4.12, dq, 8 H (OCH_2), $|^3J(^{31}\text{P-O-C-}^1\text{H})| = 10.0$, $|^3J(^1\text{H-C-C-}^1\text{H})| = 7.5$; 1.58, s, 6 H (Sn–$CH_3$), $|^2J(^{117,119}\text{Sn-C-}^1\text{H})| = 79.0, 75.0$; 1.38, t, 12 H ($CH_3$), $|^3J(^1\text{H-C-C-}^1\text{H})| = 7.5$
C_6H_5	CH_3	8.13–7.33, m, 10 H (C_6H_5–Sn); 3.48, d, 6 H (OCH_3), $|^3J(^{31}\text{P-O-C-}^1\text{H})| = 15.5$
C_6H_5	C_2H_5	8.17–7.36, m, 10 H (C_6H_5–Sn); 3.89, dq, 8 H (OCH_2), $|^3J(^{31}\text{P-O-C-}^1\text{H})| = 10.0$, $|^3J(^1\text{H-C-C-}^1\text{H})| = 7.0$; 1.16, t, 12 H ($CH_3$), $|^3J(^1\text{H-C-C-}^1\text{H})| = 7.0$
C_6H_5	*n*-C_3H_7	8.16–7.32, m, 10 H (C_6H_5–Sn); 3.73, dt, 8 H (OCH_2), $|^3J(^{31}\text{P-O-C-}^1\text{H})| = 9.5$, $|^3J(^1\text{H-C-C-}^1\text{H})| = 6.5$; 1.77–1.23, m, 8 H ($CH_2$); 0.80, t, 12 H ($CH_3$), $|^3J(^1\text{H-C-C-}^1\text{H})| = 7.0$
C_6H_5	*i*-C_3H_7	8.19–7.37, m, 10 H (C_6H_5–Sn); 4.42, m, 4 H (OCH); 1.14, d, 24 H (CH_3), $|^3J(^1\text{H-C-C-}^1\text{H})| = 6.0$
C_6H_5	*i*-C_4H_9	8.27–7.20, m, 10 H (C_6H_5–Sn); 3.53, dd, 8 H (OCH_2), $|^3J(^{31}\text{P-O-C-}^1\text{H})| = 9.0$, $|^3J(^1\text{H-C-C-}^1\text{H})| = 7.5$; 1.73, m, 4 H (CH); 0.82, d, 24 H (CH_3), $|^3J(^1\text{H-C-C-}^1\text{H})| = 7.0$
C_6H_5	C_6H_5	7.83–6.80, m, 30 H (C_6H_5–Sn, OC_6H_5)

[a] In $CDCl_3$; TMS as internal standard. [b] s = singlet, d = doublet, t = triplet, m = multiplet, dd = doublet of doublets, dt = doublet of triplets, dq = doublet of quartets.

Table IV. Infrared Frequencies (cm^{-1}) for $R_2Sn[S_2P(OR')_2]_2$ in the Range 1400–200 cm^{-1}[a,b]

R	R′	
CH_3	CH_3	1300 w, 1170 s, 1025 vs (vbr), 780 vs (br), 650 s (br), 550 sh, 495 sh, 485 m, 365 vvw, 350 vvw, 300 w, 275 w, 255 w, 215 w
CH_3	C_2H_5	1385 m, 1285 w, 1155 m, 1090 m, 1020 sh, 1005 vvs, 935 vvs, 765 vvs, 645 s (br), 540 sh, 505 m, 375 sh, 365 sh, 355 sh, 340–220 w (br) showing slight fine structure
C_6H_5	CH_3	1315 w, 1305 sh, 1165 vs, 1155 vs, 1075 vs, 1035 vvs, 1015 vvs, 975 sh, 793 vs, 785 sh, 725 m, 690 m, 653, 605 sh, 587 s, 535 m, 490 w, 440 w (br)
C_6H_6	C_2H_5	1329 w, 1295 w, 1195 vvw, 1153 m, 1090 w, 1040 s (br), 1003 vs, 947 vs, 915 sh, 810 s, 797 sh, 790 s, 782 sh, 722 m, 685 w, 635 s (br), 500 w, 470 sh, 440 w (br)
C_6H_5	*n*-C_3H_7	1335 w, 1295 w, 1250 w, 1160 sh, 1145 w, 1125 w, 1090 sh, 1050 vs, 1010 sh, 985 vvs (br), 960 sh, 900 s, 890 m, 845 vs, 830 sh, 740 sh, 725 vs, 683 s, 640 vs (br), 600 sh, 510 m (br), 445 w, 365 vvw, 355 vvw, 245 w
C_6H_5	*i*-C_3H_7	1342 w, 1307 w, 1260 vvw, 1179 m, 1145 w, 1108 w, 1002 vs, 964 vvs, 915 w, 892 m, 790 m, 738 w, 695 w, 610 mw, 520 w, 440 w
C_6H_5	*i*-C_4H_9	1290 w, 1270 w, 1155 vw (br), 1030 sh, 1015 sh, 990 vs, 960 sh, 904 w, 850 m, 820 sh, 717 w, 680 w, 660 w, 610 w (br), 535 w, 520 sh, 440 w, 410 sh, 230 vw
C_6H_5	C_6H_5	1210 w, 1187 s, 1160 s, 1070 vw, 1022 vw, 1000 vw, 985 s, 920 vs, 900 s, 783 s, 770 sh, 750 w, 745 sh, 728 m, 688 m, 665 ms, 655 ms, 570 w (br), 515 w (br), 420 vvw

[a] Recorded as Nujol mulls on KBr plates and polyethylene film. [b] vvs = very, very strong, vs = very strong, s = strong, m = medium, w = weak, vw = very weak, vvw = very, very weak, sh = shoulder, br = broad.

Table V. Mass Spectral Data for $R_2Sn[S_2P(OR')_2]_2$[a]

mass no.	rel abund	assignt
		$R = CH_3, R' = C_2H_5$
505	0.7	$CH_3Sn[S_2P(OC_2H_5)_2]_2^+$
490	0.7	$Sn[S_2P(OC_2H_5)_2]_2^{+\cdot}$
355	19.3	?
335	100.0	$(CH_3)_2SnS_2P(OC_2H_5)_2^+$
327	10.8	$355 - C_2H_4^+$
307	22.0	$(CH_3)_2SnS_2P(OC_2H_5)OH^+$
305	24.2	$SnS_2P(OC_2H_5)_2^+$
299	13.2	$355 - 2C_2H_4^+$
279	26.4	$(CH_3)_2SnS_2P(OH)_2^+$
277	26.2	$SnS_2P(OC_2H_5)OH^+$
261	11.1	$(CH_3)_2SnS_2PO^+$
249	12.4	$SnS_2P(OH)_2^+$
247	10.7	$SnS_2PO_2^+$
245	13.9	$(CH_3)_2SnS_2P^+$
231	7.6	SnS_2PO^+
215	4.9	SnS_2P^+
183	12.1	$SnSP^+$
152	4.4	SnS^+
151	7.5	SnP^+
150	3.6	$(CH_3)_2Sn^{+\cdot}$
135	5.3	CH_3Sn^+
120	2.5	$Sn^{+\cdot}$
		$R = C_6H_5, R' = C_3H_7$
623	4.5	$C_6H_5Sn[S_2P(OC_3H_7)_2]_2^+$
546	0.5	$Sn[S_2P(OC_3H_7)_2]_2^{+\cdot}$
487	67.7	$(C_6H_5)_2SnS_2P(OC_3H_7)_2^+$
445	26.5	$(C_6H_5)_2SnS_2P(OC_3H_7)(OH)^+$
403	55.6	$(C_6H_5)_2SnS_2P(OH)_2^+$
367	2.0	$C_6H_5SnS_2P(OC_3H_7)O^+$
359	6.3	?
333	7.4	$SnS_2P(OC_3H_7)_2^+$
325	30.5	$C_6H_5SnS_2P(OH)O^+$
307	7.9	$359 - C_3H_6^+$
291	8.3	$SnS_2P(OC_3H_7)(OH)^+$
281	1.5	$359 - C_6H_6^+$
261	6.3	$C_6H_5SnS_2^+$
249	16.3	$SnS_2P(OH)_2^+$
229	49.1	$C_6H_5SnS^{+\cdot}$
197	11.9	$C_6H_5Sn^+$
183	1.6	$SnSP^{+\cdot}$
120	5.0	$Sn^{+\cdot}$

[a] Only tin-containing fragments are listed; mass numbers are based upon ^{120}Sn, ^{32}S, ^{31}P, ^{16}O, ^{12}C, and ^1H.

Table VI. Amounts of Reagents and Yields for $R_2Sn[S_2P(OR')_2]_2$

		R_2SnCl_2		$NH_4S_2P(OR')_2$		yield	
R	R'	g	mol	g	mol	g	%
CH_3	CH_3	3.30	0.015	5.30	0.03	4.5	70
CH_3	C_2H_5	0.55	0.0025	1.01	0.005	1.0	80
CH_3	n-C_3H_7	3.30	0.015	6.93	0.03	7.0	82
CH_3	i-C_3H_7	2.20	0.01	4.70	0.02[a]	3.7	65
C_6H_5	C_2H_5	1.72	0.005	2.03	0.01	2.7	82
C_6H_5	n-C_3H_7	0.86	0.0025	1.17	0.005	1.2	70
C_6H_5	i-C_3H_7	1.72	0.005	2.31	0.01	3.1	88
C_6H_5	n-C_4H_9	0.86	0.0025	1.30	0.005	0.6	33

[a] In water (50 mL).

Table VII. Amounts of Reagents and Yields for $(CH_3)_2Sn[S_2P(OR')_2]_2$

	$(CH_3)_2SnCl_2$		$HS_2P(OR')_2$		yield	
R'	g	mol	g	mol	g	%
C_2H_5	2.20	0.01	3.72	0.02	3.70	71
n-C_3H_7	2.20	0.01	4.28	0.02	3.45	60
i-C_3H_7	2.20	0.01	4.28	0.02	2.20	40

of the appropriate acid ester upon the diorganotin(IV) dichloride in an ether–ethanol solvent mixture (eq 1), by the use

$$R_2SnCl_2 + 2(NH_4)S_2P(OR')_2 \rightarrow 2NH_4Cl\downarrow + R_2Sn[S_2P(OR')_2]_2 \quad (1)$$

$$R = CH_3;\ R' = CH_3,\ C_2H_5,\ n\text{-}C_3H_7,\ i\text{-}C_3H_7$$

$$R = C_6H_5;\ R' = CH_3,\ C_2H_5,\ n\text{-}C_3H_7,\ i\text{-}C_3H_7,\ n\text{-}C_4H_9$$

of an alkali metal salt of the acid ester and ethanol as the solvent (eq 2), or by the action of the acid esters themselves

$$R_2SnCl_2 + 2MS_2P(OR')_2 \rightarrow 2MCl\downarrow + R_2Sn[S_2P(OR')_2]_2 \quad (2)$$

$$M = Na;\ R = CH_3;\ R' = CH_3,\ C_2H_5,\ n\text{-}C_3H_7,\ i\text{-}C_3H_7$$

$$M = K;\ R = n\text{-}C_4H_9;\ R' = i\text{-}C_3H_7$$

upon the diorganotin(IV) oxide in benzene (eq 3). The re-

$$R_2SnO + 2HS_2P(OR')_2 \rightarrow H_2O + R_2Sn[S_2P(OR')_2]_2 \quad (3)$$

$$R = C_6H_5;\ R' = i\text{-}C_4H_9,\ C_6H_5$$

leased water is distilled azeotropically to drive the reaction forward. Syntheses 1 and 2 have been previously used to prepare the $R = n$-C_4H_9, $R' = C_2H_5$ derivative, the latter from the sodium salt.[7] The $R = n$-C_4H_9, R' = methylcyclohexyl and octylphenyl and the R = didodecyl, $R' = i$-C_3H_7 derivatives have been prepared by synthesis 2 with use of the potassium salt,[8,9] and the $R = n$-C_4H_9, R' = 2-ethylhexyl derivative has been prepared by synthesis 3.[10]

The organotin dithiophosphate esters in Table I are air stable, colorless, crystalline solids, soluble in polar and nonpolar organic solvents.

In principle, the possible structures for this series of compounds include a four-coordinated, $R_2Sn[SP(=S)(OR')_2]_2$ configuration containing monodentate dithiophosphate ester groups, but unchelated dithiophosphate systems are rare.[11] Why both the adduct $Ni[S_2P(OCH_3)_2]_2$·2,9-Me_2-1,10-phen[12] and (*O,O'*-diethyl dithiophosphato)triphenyltin(IV), $(C_6H_5)_3SnS_2P(OC_2H_5)_2$, whose structure we have recently solved as part of this series of investigations,[2] should contain monodentate dithiophosphate ester groups is not known. It is of interest that the closely related parent 1,10-phenanthroline complex of the former[12] and other corresponding trimethyltin(IV) derivatives of the latter[1] contain chelating groups. The bidentate dithiophosphate ester ligands can be either bridging or chelating, and an ionic form, $[R_2Sn]^{2+}[S_2P(OR')_2]_2^{2-}$, is also possible.

In the case of two of the derivatives, however, the crystal structures are known. Bis(*O,O'*-diethyl dithiophosphato)diphenyltin(IV) is octahedral with chelating, anisobidentate dithiophosphate ester ligands in which the two sets of tin–sulfur distances are 2.5 and 3.2 Å (the four sulfur atoms are located in the equatorial plane), and the diphenyltin system makes a C–Sn–C angle of 135°. The corresponding isopropyl ester derivative, bis(*O,O'*-diisopropyl dithiophosphato)diphenyltin(IV), $(C_6H_5)_2Sn[S_2P(OC_3H_7\text{-}i)_2]_2$, adopts a trans-octahedral configuration which is, on the other hand, extremely symmetrical with tin–sulfur distances of 2.7 Å and an angle of 180° in the diphenyltin system. These molecules are packed very tightly into their lattice such that a conversion to a bridged polymeric form could be accomplished with no further movement of the monomeric units closer together.[4]

---

(7) Lapitskii, G. A.; Granenkina, L. S.; Khokhlov, P. S.; Bliznyuk, N. K. *J. Gen. Chem. USSR (Engl. Transl.)* **1968**, *38*, 2689.

(8) Esso Research and Engineering Co., U.S. Patent 2786812, 1957; *Chem. Abstr.* **1957**, *51*, 10892*f*.

(9) Esso Research and Engineering Co., British Patent 737392, 1955; *Chem. Abstr.* **1956**, *50*, 9010.

(10) Yoshitomi Pharmaceutical Industries, Japanese Patent 15290, 1966; *Chem. Abstr.* **1966**, *65*, 20164*f*.

(11) Wasson, J. R.; Woltermann, G. M.; Stoklosa, H. J. *Fortschr. Chem. Forsch.* **1973**, *35*, 65.

(12) Shetty, P. S.; Fernando, Q. *J. Am. Chem. Soc.* **1970**, *92*, 3964.

(13) Lieblich, B. W.; Tomassini, M. *Acta Crystallogr., Sect. B* **1978**, *B34*, 944.

Table VIII. Tin-119m Mössbauer Quadrupole Splittings and the C–Sn–C Angles in Hexacoordinated Diphenyltin(IV) Compounds

compd	QS, mm s^{-1}	ref	C–Sn–C, deg	ref
$(C_6H_5)_2SnCl_2\cdot 2Me_2SO$(1a,b)[a]	3.54, 3.86	37, 39	167.2 (2),[b] 171.8 (2)[b,c]	38
$(C_6H_5)_2SnCl_2\cdot$bpy (2a,b)[a]	3.51, 3.90	37, 40	173.5 (3)[b]	41
$(C_6H_5)_2Sn[S_2CN(C_2H_5)_2]_2$ (3)[a]	1.74	42	101.4 (6)[b]	43
$(C_6H_5)_2Sn[S_2P(OC_2H_5)_2]_2$ (4)[a]	3.12	*d*	135 (1)[b]	13
$(C_6H_5)_2Sn[S_2P(OC_3H_7\text{-}i)_2]_2$ (5)[a]	3.67	*d*	180.0 (0)[b]	2
$(C_6H_5)_2Sn[S_2P(OC_6H_5)_2]_2$	3.21	*d*	142[e]	
$(C_6H_5)_2Sn[S_2P(OC_3H_7\text{-}n)_2]_2$	3.22	*d*	142[e]	
$(C_6H_5)_2Sn[S_2P(OCH_3)_2]_2$	3.34	*d*	146.5[e]	
$(C_6H_5)_2Sn[S_2P(OC_4H_9\text{-}i)_2]_2$	3.62	*d*	159.5[e]	

[a] Numbers in parentheses refer to Figure 1. [b] Estimated standard deviations in parentheses. [c] Mean values of these angles used in Figure 1. [d] This work. [e] Values predicted by using eq 1.

In all likelihood then, the series of compounds synthesized here will adopt trans-octahedral geometries with bidentate, chelating dithiophosphate ester groups as is generally found in other derivatives of the main-group and transition elements.[11]

Infrared Spectra. Infrared data cannot in any case distinguish the various structural possibilities, since it is impossible to assign with confidence the P—S and P═S stretching frequencies. For example, bands probably associated with the P—S stretching frequencies in the transition-metal complexes which contain bidentate, chelating dithiophosphate ester ligands appear in the same region as for the free acids $(RO)_2P({=}S)SH$ and their esters $(RO)_2P({=}S)SR'$.[14] There seems little sensitivity on the part of the observed frequencies at 560–530 and 670–630 cm^{-1},[15] probably corresponding to $\nu_{sym}(PS_2)$ and $\nu_{asym}(PS_2)$, respectively, to the nature of the groups connected to sulfur.[15,16]

The infrared data for our compounds are listed in Table IV. The $\nu_{sym}(PS_2)$ absorptions obscure the important ν(SnC) frequencies, which could yield information concerning the configuration of the C–Sn–C skeletons. While frequencies in the ν(CO) region are observed in the 1170–1145-cm^{-1} range, in the ν(POR) region in the 1025–985-cm^{-1} range[17] and in the $\nu(PS_2)$ region in the 660–610-cm^{-1} range for the compounds listed, none of the assignments can be made with confidence because of the richness of the spectra. The PS_2 modes have been assigned in the analogous organolead,[18] -thallium,[16] and -mercury[19] derivatives.

NMR Spectra. Chemical shifts and NMR coupling constant data are listed in Table III. Resonances which can be assigned to the phenyltin protons fall in the range 8.27–7.32 ppm; in bis(*O,O′*-diphenyl dithiophosphato)diphenyltin(IV), $(C_6H_5)_2Sn[S_2P(OC_6H_5)_2]_2$, the 30 C_6H_5Sn and OC_6H_5 protons fall in the range 7.83–6.80 ppm. The expected integrated areas and peak multiplicities for the organic ester groups attached to phosphorus through oxygen are observed in the spectra as indicated in the table. For example in the spectrum of bis(*O,O′*-dimethyl dithiophosphato)diphenyltin(IV), $(C_6H_5)_2Sn[S_2P(OCH_3)_2]_2$, the methoxy-group signal appears as a doublet arising from the coupling $|^3J(^{31}P\text{–}O\text{–}C\text{–}^1H)| = 15.5$ Hz, and in the corresponding ethoxy derivative the methylene protons appear as a doublet of quartets arising from a coupling of 10.0 Hz to the phosphorus-31 nucleus and the coupling $|^3J(^1H\text{–}C\text{–}C\text{–}^1H)| = 7.0$ Hz with the terminal methyl protons of the ethyl group. The methyltin couplings, $|^2J(^{119}Sn\text{–}C\text{–}^1H)| = 80.0$ and 79.0 Hz, respectively, for the methoxy and ethoxy esters, fall in the range expected for six-coordinated, diorganotin species in the dilute solutions in which they were recorded.[20]

Mass Spectra. The typical mass spectral data of the dimethyl- and diphenyltin dithiophosphate esters listed in Table V are quite similar. In none of the spectra is there a detectable molecular ion, nor are there any fragments of mass higher than the monomer, nor any arising from polytin species, thus ruling out any gas phase association of these monomers. The most abundant tin-bearing ion arises in each case from the loss of one of the dithiophosphate ester ligands. The successive loss of the organic groups from the tin atom is also a feature of these spectra. In addition there is the loss of alkene from the ester portion of all the dithiophosphate ligands except where $R' = CH_3$ and C_6H_5.

A reasonable pathway for the decomposition of these esters appears to be by sequential loss of alkene from those dithiophosphate groups where this is possible, after initial loss of one ligand molecule and the organic group from tin. Thus for the dimethyltin ethyl ester, prominent fragments arise at m/e 505 $[P - CH_3]^+$ and 490 $[P - 2CH_3]^+$ owing to the successive loss of methyl groups, m/e 335 $[P - S_2P(OC_2H_5)_2]^+$ and 150 $[P - 2S_2P(OC_2H_5)_2]^+$ owing to the successive loss of ligand molecules, and m/e 307 $[P - L - C_2H_4]^+$ and 279 $[P - L - 2C_2H_4]^+$ owing to the successive loss of ethylene. As in the case of the trimethyltin derivatives,[1] most of the high abundance fragments are even electron ions (see, for example, Table V).

Mössbauer Spectra. The tin-119m Mössbauer data listed in Table II can be interpreted in terms of diorganotin(IV) complexes in a six-coordinated, trans-octahedral configuration. The magnitudes of the isomer shift (IS) values (1.35–1.47 mm s^{-1}) specify a tin(IV) oxidation state. The magnitudes of the ρ values [ratio of quadrupole splitting (QS) to IS] (2.18–2.62) reflect a higher than four-coordinated situation at the tin atom, while the magnitudes of the QS values (3.12–3.67 mm s^{-1}) are indicative of a *trans*-diorganotin configuration in an octahedral geometry.[21]

The variation in the magnitude of the QS with the angle C–Sn–C for six-coordinated diorganotin compounds has been calculated from a point-charge approach[22] given by eq 4, where

$$|QS| = 4\{R\}[1 - 3 \sin^2 \theta \cos^2 \theta]^{1/2} \qquad (4)$$

$\{R\}$ = partial quadrupole splitting for group R (−0.95 mm s^{-1} for R = C_6H_5[23]) and C–Sn–C = $(180 - 2\theta)°$. The treatment assumes that there will be no sign inversion in the QS data throughout the systems compared, that the partial QS values for the ligands are small compared to that for the phenyl ligand, and that $\{C_6H_5\}$ is a constant over the compounds studied. Nevertheless, this correlation is supported by the abundant structural data for six-coordinated dimethyltin(IV)

---

(14) Chittenden, R. A.; Thomas, L. C. *Spectrochim. Acta* **1964**, *20*, 1679.
(15) Adams, D. M.; Cornell, J. B. *J. Chem. Soc. A* **1968**, 1299.
(16) Walther, B. *Z. Anorg. Chem.* **1972**, *395*, 211.
(17) Walther, B. *Z. Anorg. Chem.* **1972**, *395*, 211.
(18) Haiduc, I.; Martinas, F.; Ruse, D.; Curtui, M. *Synth. React. Inorg. Met.-Org. Chem.* **1975**, *5*, 103.
(19) Haiduc, I.; Veres, E. *Synth. React. Inorg. Met.-Org. Chem.* **1975**, *5*, 115.
(20) Petrosyan, V. S. *Prog. Nucl. Magn. Reson. Spectrosc.* **1977**, *11*, 115.
(21) Zuckerman, J. J. *Adv. Organomet. Chem.* **1970**, *9*, 21.
(22) Sham, T. K.; Bancroft, G. M. *Inorg. Chem.* **1975**, *14*, 2281.
(23) Clark, M. G.; Maddock, A. G.; Platt, R. H. *J. Chem. Soc., Dalton Trans.* **1972**, 210.

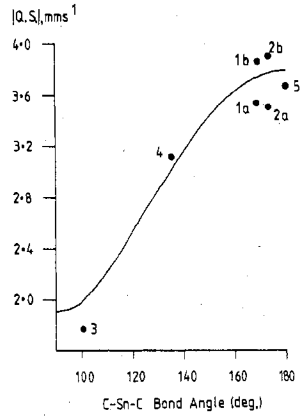

Figure 1. Correlation plot of tin-119m Mössbauer quadrupole splittings (QS) vs. the C–Sn–C angles in hexacoordinated diphenyltin(IV) derivatives.

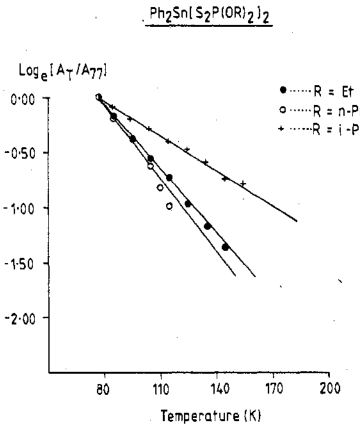

Figure 2. Plot of ln A (normalized to the area under the Mössbauer resonance curve at 77 K) vs. temperature in K. The slopes are −1.92, −2.19, and −1.06 × 10^{-2} K^{-1} for the ethyl, *n*-propyl, and isopropyl derivatives.

compounds,[22] although for the corresponding diphenyltin(IV) system surprisingly few crystal structure studies are available.[24] The data for the compounds for which both Mössbauer and phenyl–tin–phenyl C–Sn–C angles are available are plotted in Figure 1, and listed in Table VIII along with the predicted C–Sn–C angles given by the correlation expressed in eq 1 above, for the remaining diphenyltin dithiophosphates whose QS values are known.

Variable-Temperature Mössbauer Study. Three compounds have been subjected to variable-temperature Mössbauer study, and the results are depicted in Figure 2. The Mössbauer recoil-free fraction, f, is related to the mean-square displacement, $\langle x^2 \rangle$, of the tin atom from its equilibrium position by eq 5, where $\lambda\!\!\!^-$ is the wavelength of the Mössbauer γ ray

$$f = \exp[-\langle x^2 \rangle / \lambda\!\!\!^-{}^2] \qquad (5)$$

divided by 2π. For thin absorbers, with use of the Debye model, f is linearly related to the area under the Mössbauer resonance, A_T, and its temperature dependence is given by

$$A_T \propto f = \exp[-6E_R T / k\theta_D{}^2] \quad \text{for } T \geq \theta_D/2 \qquad (6)$$

where E_R is the Mössbauer recoil energy and θ_D is the Debye temperature of the solid. Thus, in the high-temperature limit, plots of ln A_T vs. temperature should be linear. It is found that the more tightly bound the tin atoms are in a lattice, the slower will be the fall in f and hence A_T, as the temperature is raised. Compounds of known structure containing noninteracting, monomeric molecules exhibit slopes [(d ln A_T)/dT)] of ca. −1.8 × 10^{-2} K^{-1}, no matter what the coordination number at tin. Weak intermolecular interactions such as hydrogen bonding reduce this value to ca. −1.7 × 10^{-2} K^{-1}, while a more complex system of hydrogen bonds can reduce it further to ca. −1.3 × 10^{-2} K^{-1}. Strongly hydrogen-bonded lattices and solids in which one-, two-, or three-dimensional association is present exhibit slopes of ca. −0.9 × 10^{-2} K^{-1}. The lowest value, −0.23 × 10^{-2} K^{-1}, is given by tin(II) oxide.[25-28]

According to these systematics, the magnitudes of the slopes of the plots of ln A_T vs. temperature for the ethyl (−1.92 × 10^{-2} K^{-1}) and *n*-propyl (−2.19 × 10^{-2} K^{-1}) esters correspond to an arrangement of noninteracting monomeric molecules in the solid. The X-ray crystal structure of the ethyl derivative which is a badly distorted octahedral complex of tin is corroboratory, and it is likely from the magnitudes of both the slope in Figure 2 and the QS (3.12 vs. 3.22 mm s^{-1}) that the *n*-propyl analogue is roughly isostructural in being a six-coordinated, distorted octahedron with a C–Sn–C angle essentially the same (142°) as found in the ethyl derivative (vide supra). Comparison can be drawn with the corresponding slope data for tetraphenyltin(IV), −1.659 × 10^{-2} K^{-1},[29,30] for which a Mössbauer spectrum at room temperature can be resolved.[31]

The isopropyl ester derivative, $(C_6H_5)_2Sn[S_2P(OC_3H_7\text{-}i)_2]_2$, stands as an exception to the systematics thus far developed in correlating the slope data vs. structure. The magnitude of −1.06 × 10^{-2} K^{-1} may be interpreted in terms of an associated solid into which tin atoms are bound in a one-, two-, or three-dimensional polymeric lattice. Instead, the X-ray crystal structure reveals an arrangement of symmetrical, octahedral monomers in which there are very short sulfur–sulfur atom contact distances which define an axis of propogation through the crystal. The tin–tin atom distances along this axis (6.34 Å) are such that pairs of metal atoms could be bridged by the dithiophosphate ligands without significantly altering the bite distance between the sulfur atoms. Thus the ligands could be shifted along the axis from a chelating position to a bridging position with no change in internuclear distances or for that matter in the density of the resulting solid. We have termed this situation a "virtual polymer".[4] Care must, therefore, be exercised in interpreting this type of slope information in terms of molecular structure.

Effective Vibrating-Mass Model. This treatment combines data from the variation of the recoil-free fraction with temperature with the low-energy (<200 cm^{-1}) lattice mode absorptions in the Raman spectrum to yield the mass of the vibrating unit in the solid.[32] The molecularity of the vibrating unit is calculated from eq 7, where (d ln A)/dT is the slope

$$M_{\text{eff}} = -\frac{3E_\gamma{}^2 k}{(hc)^2 \omega_L{}^2} \left(\frac{dT}{d \ln A} \right) \qquad (7)$$

of the plot of the normalized area under the Mössbauer resonance vs. temperature for which data for three compounds have been discussed above and E_γ is the energy (23.8 keV)

---

(24) Zubieta, J. A.; Zuckerman, J. J. *Prog. Inorg. Chem.* **1978**, *24*, 251.

(25) Harrison, P. G.; Phillips, R. C.; Thornton, E. W. *J. Chem. Soc., Chem. Commun.* **1977**, 603.

(26) Harrison, P. G.; Molloy, K. C.; Thornton, E. W. *Inorg. Chim. Acta* **1978**, *33*, 137.

(27) Harrison, P. G.; Begley, M. J.; Molloy, K. C. *J. Organomet. Chem.* **1980**, *186*, 213.

(28) Herber, R. H.; Leahy, M. F. *J. Chem. Phys.* **1977**, *67*, 2718.

(29) Reported as −1.60 × 10^{-2} K^{-1} in ref 30.

(30) Hazony, Y.; Herber, R. H. In "Mössbauer Effect Methodology"; Gruverman, I., Seidel, C. W., Eds.; Plenum Press: New York, 1978; Vol. 8, p 107.

(31) Bancroft, G. M.; Butler, K. D.; Sham, T. K. *J. Chem. Soc., Dalton Trans.* **1975**, 1483.

(32) Herber, R. H.; Leahy, M. F. *Adv. Chem. Ser.* **1976**, No. *157*, 155.

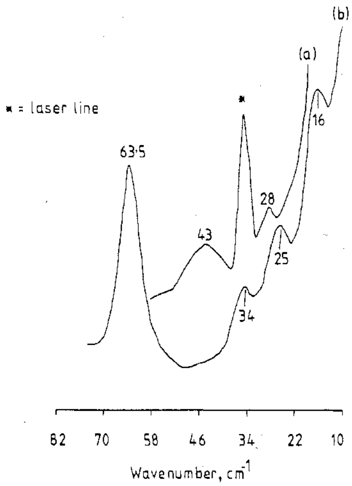

Figure 3. Low-energy, lattice-mode Raman spectra of (a) bis(*O*,*O'*-diethyl dithiophosphato)diphenyltin(IV) using a 488.0-nm laser source and (b) bis(*O*,*O'*-diisopropyl dithiophosphato)diphenyltin(IV) using a 476.5-nm laser source, both at 100 mW.

Table IX. Low-Energy, Lattice-Mode Raman Frequencies and M_{eff} Values from the Effective Vibrating-Mass Model

compd	ω	M_{eff}	mol wt multiple
$(C_6H_5)_2Sn[S_2P(OC_2H_5)_2]_2$ (mol wt 643.37)	28	680	1.06
	43	289	0.45
	58	159	0.25
$(C_6H_5)_2Sn[S_2P(OC_3H_7\text{-}i)_2]_2$ (mol wt 699.49)	16	3793	5.42
	25	1546	2.21
	34	836	1.20
	63.5	240	0.34
	88	125	0.18

of the Mössbauer γ ray. The low-energy Raman spectra which should contain the frequency, ω, are shown in Figure 3 for the ethyl and isopropyl ester derivatives.

The spectrum of the *n*-propyl derivatives lacks bands which could be reasonably assigned to this mode. This has been noted in the case of $[Sn(SCH_2CH_2S)_2]_n$ where the mode sought is only observable at low temperature (77 K).[31] The molecular weights of the ethyl and isopropyl monomers are 643.37 and 699.49, respectively. Thus no band in either spectrum above those found at 28 and 34 cm^{-1}, respectively, can correspond to the unique, intermolecular, intra unit cell vibration sought in this treatment. The 28-cm^{-1} band in the spectrum of the ethyl ester derivative corresponds closely, as can be seen from the data displayed in Table IX, to the monomer, but the 34-cm^{-1} band for the isopropyl analogue is in only moderate agreement with its corresponding monomer value. In this latter case the bands at 25 and 16 cm^{-1} must also be considered, and a polymeric structure cannot be ruled out. The X-ray crystal structure information discussed above is corroboratory, and the description in terms of a "virtual polymer" is thus not unreasonable.[4]

Table X. Temperature Dependence of Mössbauer Spectral Areas for $(C_6H_5)_2Sn[S_2P(OC_2H_5)_2]_2$

T, K	$A_+{}^a$	$A_-{}^a$	$A_{\mathrm{total}}(T)$	$R = A_+/A_-$
77	0.078	0.088	0.167	0.898
85	0.066	0.074	0.140	0.892
95	0.053	0.061	0.114	0.869
105	0.044	0.051	0.095	0.863
115	0.035	0.045	0.080	0.778
125	0.028	0.035	0.063	0.800
135	0.023	0.028	0.051	0.821
145	0.015^b	0.028^b	0.043	0.536^b

^{a} A_+ and A_- are the areas under the higher (more positive) and lower velocity components in the doublet spectrum, respectively. ^{b} These values are obviously erroneous and arise from inaccurate resolution of the total resonance into its components; $A_{\mathrm{total}}(145)$ is, however, consistent with the other $A_{\mathrm{total}}(T)$ data.

Table XI. Temperature Dependence of the Mössbauer Spectral Areas for $(C_6H_5)_2Sn[S_2P(OC_3H_7\text{-}i)_2]_2$

T, K	$A_+{}^a$	$A_-{}^a$	$A_{\mathrm{total}}(T)$	$R = A_+/A_-$
77	0.061	0.062	0.123	0.984
85	0.054	0.058	0.112	0.931
95	0.047	0.053	0.100	0.887
105	0.043	0.049	0.092	0.878
115	0.039	0.043	0.082	0.907
125	0.036	0.041	0.077	0.878
135	0.031	0.038	0.069	0.816
145	0.027	0.031	0.058	0.871
155	0.024^b	0.032^b	0.056	0.750^b

^{a} A_+ and A_- are the areas under the higher (more positive) and lower velocity components of the doublet spectrum, respectively. ^{b} These values are obviously erroneous and arise from inaccurate resolution of the total resonance into its components. $A_{\mathrm{total}}(155)$ is, however, consistent with all other $A_{\mathrm{total}}(T)$ data.

Temperature Variation of the Goldanskii–Karyagin Effect. The anisotropy of the Mössbauer recoil-free fraction, commonly called the Goldanskii–Karyagin effect[33,34] and observed as an asymmetry of the relative intensities of the two lines of a doublet spectrum, can also yield information concerning the lattice dynamics of solids, especially if X-ray diffraction data are also available. In our case the structures of both the ethyl and isopropyl derivatives are available, and the trans C–Sn–C axis can be defined as the z axis by analogy with the published treatment of $(CH_3)_2Sn(C_5H_7O_2)_2$,[35] whose structure is also known.[36] For $(C_6H_5)_2Sn[S_2P(OC_2H_5)_2]_2$, the z axis is defined as the idealized C–Sn–C axis in which this vector is linear. The motion perpendicular to the axis for both esters lies in the plane of the two chelating ligands. In cases such as this it is possible to derive from the Mössbauer data two separate, effective Debye temperatures corresponding to the motion of the tin atom parallel and perpendicular to this axis. The combined effect of the anisotropies in the electric charge density and the force constants results in the temperature-dependent asymmetry of the Mössbauer doublet. The ratio of the areas of the two wings of the doublet can then be related to the mean-square vibrational amplitudes parallel and perpendicular to the symmetry axis if the shape of the electric charge distribution about the tin atom is known. From previous X-ray[24] and Mössbauer[35] studies it is known that the motion of the tin atom is more constrained in the equatorial plane of octahedral, *trans*-diorganotin complexes than along the C–Sn–C bonds, and in the two compounds for which structural data are available the two components of the Mössbauer resonance doublet are easily resolved and the areas measured (Tables X and XI), and large resonance effects are observed even for thin absorbers. It is possible to obtain information about the mean-square amplitudes of vibration parallel ($\langle x_\parallel{}^2\rangle$) and perpendicular ($\langle x_\perp{}^2\rangle$) to the z axis by measuring the temperature dependence of the areas of the two resonance lines. Plots of the temperature dependence of $\langle x_\parallel{}^2\rangle$ and $\langle x_\perp{}^2\rangle$ for the ethyl and isopropyl ester derivatives are shown in Figures 4 and 5, respectively. The description of the treatment follows.

---

(33) Greenwood, N. N.; Gibb, T. C. "Mössbauer Spectroscopy"; Chapman and Hall: London, 1971.
(34) Gibb, T. C. "Principles of Mössbauer Spectroscopy"; Chapman and Hall: London, 1976.
(35) Herber, R. H.; Leahy, M. F.; Hazony, Y. *J. Chem. Phys.* **1974**, *60*, 5070.
(36) Miller, G. A.; Schlemper, E. O. *Inorg. Chem.* **1973**, *12*, 677.

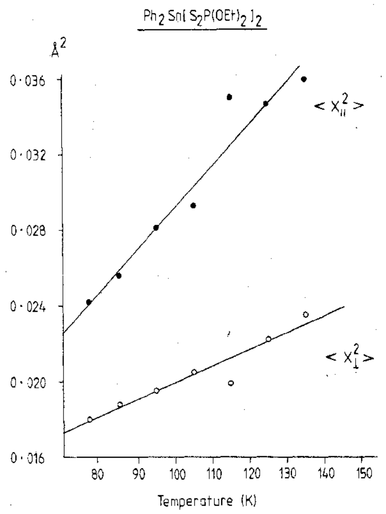

Figure 4. Temperature-dependence of $\langle x_\parallel^2\rangle$ and $\langle x_\perp^2\rangle$ in Å^2 between 77 and 135 K for bis(*O,O′*-diethyl dithiophosphato)diphenyltin(IV).

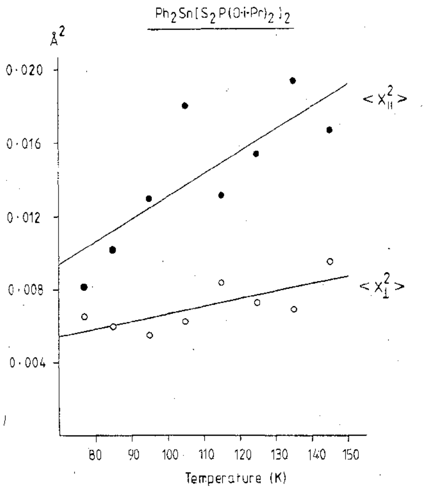

Figure 5. Temperature-dependence of $\langle x_\parallel^2\rangle$ and $\langle x_\perp^2\rangle$ in Å^2 between 77 and 145 K for bis(*O,O′*-diisopropyl dithiophosphato)diphenyltin(IV).

As in the case of dimethyltin(IV) bis(acetylacetonate)[35] we assume a prolate shape for the electrostatic field about the z axis of cylindrical symmetry (C–Sn–C) and hence that V_{zz}, the principal component of the electric field gradient tensor, is negative. A prolate field acting on a tin-119m nucleus moves the spin $^3/_2$ level to higher energy with respect to the spin $^1/_2$ level, and R (the ratio of the area under the more positive velocity component of the quadrupole doublet to the area of the more negative component $= A^+/A^- = A_\pi/A_\sigma$. Consequently, the doublet component at higher velocities corresponds to the $\Delta m = \pm 1$ (π) transition and the lower one to the $\Delta m = 0$ (σ) transition. In the *trans*-diorganotin octahedra studied here, the bulk of the electron density would be expected to lie along the C–Sn–C axis, and hence a prolate field and negative V_{zz} are reasonable.

The mean-square amplitudes of vibration parallel and perpendicular to V_{zz} can be expressed as

$$A \propto \ln f = -(1/3\bar{\lambda}^2)[2\langle x_\parallel^2\rangle + \langle x_\perp^2\rangle] \tag{8}$$

or in terms of an asymmetry factor, ϵ, where

$$\epsilon = [\langle x_\parallel^2\rangle - \langle x_\perp^2\rangle]/\bar{\lambda}^2 \tag{9}$$

and hence

$$\langle x_\parallel^2\rangle = \bar{\lambda}^2(2\epsilon/3 - \ln f) \tag{10}$$

and

$$\langle x_\perp^2\rangle = -\bar{\lambda}^2(\epsilon/3 + \ln f) \tag{11}$$

Of the four variables in these latter two equations, $\epsilon, f, \langle x_\parallel^2\rangle$ and $\langle x_\perp^2\rangle$, ϵ can be calculated from the temperature dependence of A_π/A_σ and f from the temperature dependence of the total area under the resonance plus one value of f. This latter value may be derived indirectly from the X-ray thermal data at the temperatures at which the crystal structures were determined (298 K for the ethyl ester and 138 K for the isopropyl ester derivative) by using eq 5.

The temperature dependence of the total area is used to generate the data used to construct Figures 4 and 5. It is seen that since $R < 0$, the asymmetry parameter, ϵ, is always positive; that is, $\langle x_\parallel^2\rangle > \langle x_\perp^2\rangle$ in the temperature range measured.[37] The equations of the two plots for the ethyl ester are

$$\langle x_\parallel^2\rangle = 2.21 \times 10^{-4}T + 7.13 \times 10^{-3} \tag{12}$$

(correlation coefficient 0.969, number of points 7, in the temperature range 77–135 K) and

$$\langle x_\perp^2\rangle = 8.66 \times 10^{-5}T + 1.12 \times 10^{-2} \tag{13}$$

(correlation coefficient 0.951, number of points 7, in the temperature range 77–135 K). The corresponding plots for the isopropyl ester are

$$\langle x_\parallel^2\rangle = 1.28 \times 10^{-4}T + 2.56 \times 10^{-4} \tag{14}$$

(correlation coefficient 0.811, number of points 8, in the temperature range 77–145 K) and

$$\langle x_\perp^2\rangle = 4.17 \times 10^{-5}T + 2.47 \times 10^{-3} \tag{15}$$

(correlation coefficient 0.730, number of points, 8, in the temperature range 77–145 K). The mean-square amplitudes of vibration from the Mössbauer experiment for the ethyl ester are 1.80×10^{-2} and 2.42×10^{-2} Å^2 for $\langle x_\perp^2\rangle$ and $\langle x_\parallel^2\rangle$, respectively, at 77 K and 2.35×10^{-2} and 3.60×10^{-2} Å^2 at 135 K. The corresponding data for the isopropyl analogue are 0.65×10^{-2} and 0.81×10^{-2} Å^2 at 77 K and 0.68×10^{-2} and 1.94×10^{-2} Å^2 at 135 K for direct comparison.

From these observations we can see that, while both the $S_2P(OR')_2$ ligands chelate their respective tin atoms, the $R' =$ isopropyl ester ligand does so more tightly, giving rise to $\langle x_\perp(T)^2\rangle_{C_2H_5} \gg \langle x_\perp(T)^2\rangle_{C_3H_7\text{-}i}$ for all T values measured and also $\mathrm{d}\langle x_\perp(T)^2\rangle_{C_2H_5}/\mathrm{d}T > \mathrm{d}\langle x_\perp(T)^2\rangle_{C_3H_7\text{-}i}/\mathrm{d}T$. The "virtual polymer" nature of the $R = i\text{-}C_3H_7$ lattice which propagates along a plane containing the $Sn[S_2P(OC_3H_7\text{-}i)]_2$ units also contributes to this effect.

In addition, while for $R' = i\text{-}C_3H_7$ the angle C–Sn–C is 180° so that the bulky phenyl group lies along the z axis, for the $R' = C_2H_5$ structure these atoms make an angle of only 135° and hence do not lie completely along the axis. This fact helps to explain why $\langle x_\parallel(T)^2\rangle_{C_2H_5} \gg \langle x_\parallel(T)^2\rangle_{C_3H_7\text{-}i}$ and $\mathrm{d}\langle x_\parallel(T)^2\rangle_{C_2H_5}/\mathrm{d}T > \mathrm{d}\langle x_\parallel(T)^2\rangle_{C_3H_7\text{-}i}/\mathrm{d}T$. Both factors contribute to the difference in the slopes of the area under the Mössbauer resonance vs. temperature plots which are -1.06×10^{-2} K^{-1}

---

(37) Flinn, P.; Ruby, S. L.; Kehl, W. L. *Science (London)* **1964**, *143*, 1434.
(38) Poller, R. C.; Ruddick, J. N. R.; Taylor, B.; Toley, D. L. B. *J. Organomet. Chem.* **1970**, *24*, 341.
(39) Coghi, L.; Nardelli, M.; Pelizzi, C.; Pelizzi, G. *Gazz. Chim. Ital.* **1975**, *105*, 1187.
(40) Liengme, B. V.; Randall, R. S.; Sams, J. R. *Can. J. Chem.* **1972**, *50*, 3212.
(41) Parish, R. V.; Platt, R. H. *Inorg. Chim. Acta* **1970**, *4*, 65.
(42) Harrison, P. G.; King, T. J.; Richards, J. A. *J. Chem. Soc., Dalton. Trans.* **1976**, 2317.
(43) Thompson, D. W.; Barrett, P. B.; Lefelhocz, J. F.; Lock, G. A. *J. Coord. Chem.* **1973**, *3*, 119.
(44) Lindley, P. F.; Carr, P. *J. Cryst. Mol. Struct.* **1974**, *4*, 173.

for R′ = C_3H_7-*i* and -1.92×10^{-2} K^{-1} for R′ = C_2H_5.

The calculation of absolute values of mean-square amplitudes of vibration is based upon knowledge of one value of *f*, which is in this treatment derived from a known value of $\langle x^2 \rangle$ obtained from the X-ray data. Since this latter parameter in the X-ray experiment has inherent and undeterminable errors, the calculated values of $\langle x_\perp^2 \rangle$ and $\langle x_\parallel^2 \rangle$ will propagate this error and are thus quoted only as a guide to the relative changes in the directional amplitudes of motion of the Mössbauer atom. However, the temperature coefficients of these vibrations (i.e., the slopes of the lines in Figures 4 and 5) are independent in this treatment of an absolute value of *f* and hence the need for $\langle x^2 \rangle$ from the X-ray data. The coefficients are characteristic of the two samples studied and enable comparison of the chelating power of the dithiophosphate ligands. This treatment is capable of extension to other chelating systems, where it can serve to measure the relative binding powers of the ligands without having X-ray data available.

Acknowledgment. Our work is supported by the Office of Naval Research and by the National Science Foundation through Grant CHE-78-26584. We thank M&T Chemicals, Inc., for the donations of organotin starting materials and Professor R. E. Frech of the University of Oklahoma for help with the Raman spectra.

Registry No. $(CH_3)_2Sn[S_2P(OCH_3)_2]_2$, 74096-98-3; $(CH_3)_2Sn[S_2P(OC_2H_5)_2]_2$, 74096-99-4; $(CH_3)_2Sn[S_2P(O\text{-}n\text{-}C_3H_7)_2]_2$, 74097-00-0; $(CH_3)_2Sn[S_2P(O\text{-}i\text{-}C_3H_7)_2]_2$, 74097-01-1; $(C_6H_5)_2Sn[S_2P(OCH_3)_2]_2$, 74097-02-2; $(C_6H_5)_2Sn[S_2P(OC_2H_5)_2]_2$, 74097-03-3; $(C_6H_5)_2Sn[S_2P(O\text{-}n\text{-}C_3H_7)_2]_2$, 74097-04-4; $(C_6H_5)_2Sn[S_2P(O\text{-}i\text{-}C_3H_7)_2]_2$, 73453-95-9; $(C_6H_5)_2Sn[S_2P(O\text{-}n\text{-}C_4H_9)_2]_2$, 74097-05-5; $(C_6H_5)_2Sn[S_2P(O\text{-}i\text{-}C_4H_9)_2]_2$, 74097-06-6; $(C_6H_5)_2Sn[S_2P(OC_6H_5)_2]_2$, 74097-07-7; $(CH_3)_2SnCl_2$, 753-73-1; $(C_6H_5)_2SnCl_2$, 1135-99-5; $(C_6H_5)_2SnO$, 2273-51-0.

Contribution from the Chemistry Department,
University of Virginia, Charlottesville, Virginia 22901

Coordination of Adenosine Monophosphate and Inosine Monophosphate to dienPd^{2+} and enPd^{2+} [1]

IMRE SOVAGO[2] and R. BRUCE MARTIN*

Received December 26, 1979

dienPd^{2+} exhibits nearly equal tendencies to react with N(1) and N(7) of AMP. Excess dienPd^{2+} results in formation of a binuclear complex with Pd(II) at both N(1) and N(7). With two available coordination positions, enPd^{2+} reacts with N(1) of one AMP and N(7) of another. Compared to the free ligand at pH 6 downfield shifts occur for the H(8), H(2), and the ribose H(1′) protons. The 0.9-ppm downfield shift for the last proton is unusual. The binding of dienPd^{2+} to inosine is pH dependent, N(7) being favored below pH 5.5 and N(1) above that pH. With both inosine and IMP, excess dienPd^{2+} yields a binuclear complex. With IMP, enPd^{2+} reacts with both N(7) and N(1) to yield at pH 8 chemical shift differences similar to those for the AMP complex. enPd^{2+} induces a base stacked structure in inosine, IMP, GMP, and AMP.

There is a dichotomy in the binding of metal ions to the nucleic base portion of purine nucleosides and nucleotides. Both N(1) in the six-membered ring and N(7) in the imidazole ring of adenosine, inosine, and guanosine serve as donors to metal ions in solution.[3] In the nucleoside monophosphates the pK_a at N(1) is about 3.8 for adenosine, 8.9 for inosine, and 9.4 for guanosine. Thus above pH 5 the relative binding of metal ions to N(1) and N(7) is pH independent for adenosine but remains pH dependent for the 6-oxo nucleosides throughout most of the usual pH scale.[3]

As more reactive counterparts for the antitumor Pt(II) complexes, we have employed Pd(II) complexes which react more readily[4,5] and are not bedeviled by formation in neutral solutions of dihydroxo-bridged dimers which are more inert than mononuclear complexes.[6] With one coordination position available about the tetragonal metal ion, dien$Pd(H_2O)^{2+}$ in equimolar solutions favors 5:1 N(1) to N(7) binding to adenosine.[5] When the Pd to adenosine molar ratio reaches 2.0, both N(1) and N(7) sites are occupied in a binuclear complex. The ready accessibility of binuclear complexes suggests the possibility of polymer formation in necessarily *cis*-en$Pd(H_2O)_2^{2+}$ in its reactions with purine nucleosides. This possibility is explored in this paper.

There has not been agreement on the structures resulting from the reactions of Pd(II) and Pt(II) compounds with guanosine, inosine, and their derivatives. Direct five-membered ring chelation between N(7) and O(6) has been claimed.[7] The evidence, however, for this mode of interaction is not compelling, and alternative interpretations of the results are at least as plausible. For example, rather than being indicative of a strong Pd–O(6) bond,[7] the shift of an inosine band from 1700 to 1625 cm^{-1} may also be interpreted as due to deprotonation at N(1),[8] which is admitted to occur.[7] Once deprotonated, N(1) becomes the most basic site and should bind most metal ions more strongly than N(7).[3] At pH 9.7 two guanosine molecules easily bind via N(1) to the pair of available coordination positions of dmenPd^{2+}.[4] This result indicates that any chelating tendencies in guanosine must be quite weak.

Many complexes with purported N(7),O(6) chelation occur as precipitates.[7] This in itself suggests an alternative structure involving polymer formation via metal ion binding to both N(7) and N(1) of purine bases. Polymer formation has been suggested to occur in neutral solutions of *cis*-$(NH_3)_2Pt^{2+}$ and either inosine[9] or guanosine[10] by means of Raman spectra.

---

(1) This research was supported by grants from the National Cancer Institute (CA-14832) and from the National Science Foundation.

(2) On leave from the Institute of Inorganic and Analytical Chemistry, L. Kossuth University, Debrecen, Hungary.

(3) R. B. Martin and Y. H. Mariam, *Met. Ions Biol. Syst.*, **8**, 57 (1979).

(4) D. J. Nelson, P. L. Yeagle, T. L. Miller, and R. B. Martin, *Bioinorg. Chem.*, **5**, 353 (1976).

(5) M. C. Lim and R. B. Martin, *J. Inorg. Nucl. Chem.*, **38**, 1915 (1976).

(6) M. C. Lim and R. B. Martin, *J. Inorg. Nucl. Chem.*, **38**, 1911 (1976).

(7) G. Pneumatikakis, N. Hadjiliadis, and T. Theophanides, *Inorg. Chem.*, **17**, 915 (1978); *Inorg. Chim. Acta* **22**, L1 (1977); N. Hadjiliadis and T. Theophanides, *ibid.*, **16**, 77 (1976); N. Hadjiliadis and G. Pneumatikakis, *J. Chem. Soc., Dalton Trans.*, 1691 (1978).

(8) W. Beck and N. Kottmair, *Chem. Ber.*, **109**, 970 (1976).

(9) G. Y. H. Chu and R. S. Tobias, *J. Am. Chem. Soc.*, **98**, 2641 (1976).

0020-1669/80/1319-2868$01.00/0